Anisotropy of the Space Orientation of Radio Sources. II: The Axis Distribution Function

V. R. Amirkhanyan[1]

[1]*Sternberg Astronomical Institute, Universitetskii pr. 13, Moscow, 119992 Russia*
(Received March 23, 2009; Revised May 20, 2009)

An analysis of the position angles distribution of 10461 extended radio sources shows that the spatial orientation of the axes of these objects is anisotropic: they avoid the direction towards the Celestial Pole and are mostly oriented in the equatorial direction. The ratio of the probability densities of the orientation in these two directions is 0.68. The probability that the sky distribution of axes is isotropic is less than 0.00004. This conclusion is consistent with the results of the analyses of spatial distribution of galactic normals orientation in the galaxies from the UGC, ESO, and FGC catalogs.

1. INTRODUCTION

Reinhardt was the first to study the spatial orientation of galaxies over the entire sky [1]. He used the catalog of galaxies compiled by Brawn [2], a pioneer of such investigations. Reinhardt showed that the position angles distribution of the major axes of galaxies is not equiprobable and that the tilts of galaxies with respect to the observer's line of sight are inconsistent with the hypothesis of equiprobable distribution of galaxy normals orientation. The next, very important step, was made by Peter Nielson, who not only compiled the extensive Uppsala catalog of galaxies of the Northern Hemisphere [3], but also showed with high statistical significance that the distribution of position angles of galaxies is not equiprobable [4]. Lauberts extended the search for galaxies to the Southern Hemisphere and compiled the ESO catalog [5]. He analyzed the orientation of UGC and ESO objects to construct the probability density function of galaxy normals spatial orientation in form of a three-dimensional ellipsoid. Two axes of the ellipsoid with the lengths of 1 and 0.933 lie practically in the equatorial plane. The third, shortest, axis (0.778) points towards the Celestial Pole. Mandzhos et al. [6], too, analyzed the orientation of UGC and ESO galaxies and showed that the cylindrical model of spatial orientation agrees best with observations. The axis of the cylinder, perpendicularly to the lateral surface of which the galactic normals are preferentially oriented, points towards the Celestial Pole. Parnovsky et al. [7], apart from the UGC and ESO objects, included into the analysis their FGC catalog of edge-on galaxies, and showed with high statistical significance that the spatial orientation of galaxy normals is anisotropic: there are zones of avoidance (Celestial Pole) and zones of preferred orientation (the equator). Thus the above authors demonstrated convincingly that the spatial distribution of galaxy normals is anisotropic. Note that normals concentrate towards the equator and avoid the direction towards the Celestial Pole. Such a surprising coincidence is alarming. It is worthwhile to test this result on an independent sample of objects. That is why we compiled, based on the FIRST survey, a catalog of extended radio sources [9], the orientations of which we analyze in this paper.

2. SPATIAL DISTRIBUTION OF AXES. THE EXPERIMENT

Extended radio sources have a uniform structure with a well-defined axis. Modern radio telescopes produce bona fide images of radio sources out to several tens of thousands of Mpc, whereas galaxies can be properly imaged out only to about 200 Mpc; at greater distances, the errors of the geometric parameters of galaxies inferred from their image increase substantially. In [9, Fig. 7c] we constructed the position angle histogram of the catalogue radio sources. It follows from this histogram that the probability that the distribution of angles is equiprobable is less than 10^{-7}. The evident conclusion is that the spatial orientation of radio sources is anisotropic. The inverse statement is, generally speaking, not true: a "flat" distribution of position angles with respect to the Celestial Pole does not prove the absence of anisotropy of spatial orientation. Our current knowledge is insufficient to determine the spatial orientation of a particular radio source, and we can only record the celestial projection of its structure. Hence we have at our disposal the information about the coordinates of the radio sources, and the position angles of their projections with respect to the Celestial Pole. We need to reconstruct the one-dimensional distribution of position angles into a two-dimensional distribution of axes of the radio sources. Let us make the two following obvious statements:

(1) if there is a celestial direction of "preferred orientation" of the radio sources, then the distribution function of position angles with respect to this point should have the maximum non-uniformity, as compared to the distributions of position angles with
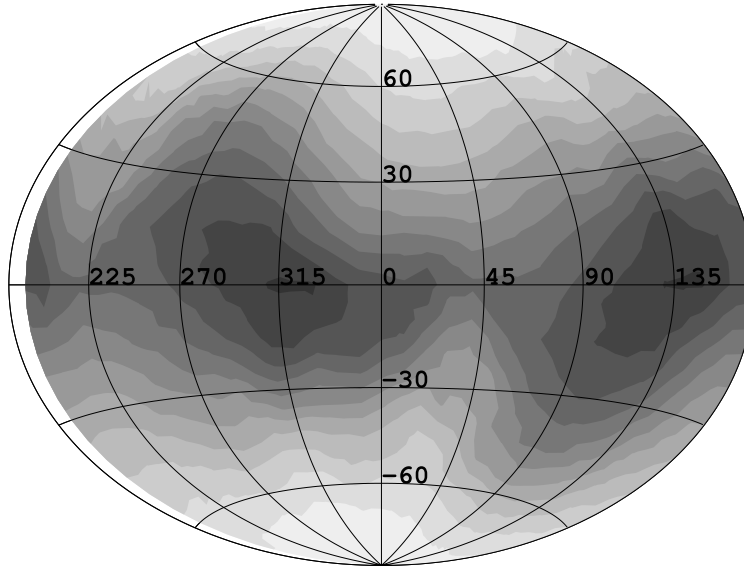
Figure 1. Experimental map of the non-uniformity of the radio sources' position angles distribution. Transition from light to dark shades corresponds to the change of the map level from the minimum towards the maximum.

respect to the neighboring points. Note that the maximum and minimum of the function are close to the zero and 90° position angles, respectively;

(2) if there is a direction in the sky, which the orientations of radio sources "tend to avoid", then the distribution function of position angles with respect to this point should have the maximum non-uniformity and the maximum and minimum of the function should be close to the 90° and zero position angles, respectively.

The more objects tend (or avoid) to orient themselves towards a certain direction, the greater is the non-uniformity of the histogram of position angles measured with respect to this direction. These are the underlying ideas of the organization of the algorithm used to construct the distribution function of the spatial orientation of the axes. The **aniso-real** program moves a point over the sky and, based on the "knowledge" of the coordinates and position angles of the radio sources of the catalog [9], computes their position angles with respect to the current point, draws the histogram of angles, and computes its parameters. We characterize the non-uniformity of the histogram by the amplitude S of its convolution with a single period of the $\cos(2p)$ harmonics, where p is the position angle counted in the interval from 0 to 180 degrees. It is clear from the above that the convolution reaches its positive and negative extrema at the point of the preferred orientation and at the point of avoidance, respectively. To pass to the amplitude of non-uniformity, we normalize the convolution to

$$W = \sum_{i=0}^{n-1} \cos^2(2\pi i/n), \qquad (1)$$

where n is the number of bins in the histogram. The program yields the map of the sky (in equatorial coordinates), where the count at each point is equal to the non-uniformity amplitude of the position angles histogram of all the catalog's radio sources with respect to the given point (Fig. 1). In this map, the transition from lighter to darker shades corresponds to a change of level from the minimum towards the maximum. Figures 2a and 2b show the histograms at the extreme points of the map. The negative extremum is located at (120°, 80°) and its level is – 53.4. The non-uniformity of the histogram at the point of the positive extremum (140°, 0°) is equal to 46.2. The dotted line shows the average level and the error bar computed assuming that the distribution of position angles is equiprobable. The probability that the histograms at the extreme points represent a "flat" distribution is less than 10^{-7}. Figure 3 shows the cross section of the map along the 130° meridian (the solid line). The dotted line shows the cross section of isotropic distribution. Its radius is equal to 581.17, i.e., the average number of radio sources per histogram bin. The deviation of isotropy is characterized by the amplitude of non-uniformity of the histograms. In this figure, the y- and x-axes correspond to the Polar axis and the equatorial plane, respectively. The map in Fig. 1 demonstrates that the axes of radio sources are preferentially oriented towards the equatorial region and avoid the direction towards the Celestial Pole. This surprising re-

sult agrees with at least equally surprising results based on the studies of UGC, ESO, and FGC galaxies. To check the operation of the **anisoreal** program, we repeated the same computations for objects of the Flat Galaxies Catalogue, that analyzed in earlier paper [7]. As a result, we obtained a map of non-uniformity of the normals position angle distribution of these objects (Fig. 4). This map shows that galactic normals, like the axes of radio sources, avoid the direction towards the Celestial Pole and prefer the equatorial region, matching the results of Parnovsky et al. [7].

3. SPATIAL DISTRIBUTION OF AXES. THE MODEL

To associate the resulting map with real anisotropy, let us construct a model of anisotropy and learn how to estimate its parameters. Here is the sequence of operations:

(1) we generate a list of the coordinates of 10461 objects uniformly distributed over the sky. We can also use the coordinates of the objects of the real catalog [9];

(2) we choose the following simple function of the spatial distribution of the axes defined by the formula:

$$P(\varphi, \omega)d\varphi d\omega = \frac{1 + A\cos^2\omega}{\pi(1 + A/2)}d\varphi d\omega. \qquad (2)$$

Here ω is the angle between the plane perpendicular to the anisotropy axis, and the axis of the radio source. For any ω the distribution in the second coordinate φ is uniform within the interval from 0 to 2π. Hence the direction $\omega = \pm\pi/2$ is the symmetry axis of the model, which can point to any direction (α_o, δ_o) in the sky. If $A < 0$, the maximum of the distribution function lies on the symmetry axis, and the minimum is located at $\omega = 0$ for $\varphi = 0$–2π. If $A > 0$, the maximum and minimum replace each other. If $A = 0$, the function $P(\varphi, \omega) = \frac{1}{\pi}$ is isotropic. The dashed line in Fig. 3 shows the cross section of function (2). For the function to fit the scale of Fig. 3, we normalized it by $\frac{1}{581.17\pi}$;

(3) for each radio source, in accordance with distribution (2) we generate the coordinates (α_i, δ_i) of the direction in the sky the axis of the source is pointed at. As a result we obtain the map of the spatial orientation of these axes;

(4) given the coordinates of the radio sources and the orientations of their axes, we compute the position angles of the axes of the radio sources with respect to the Celestial Pole;

(5) we generate the catalog of the coordinates and position angles of objects;

(6) we run the **anisoreal** code to analyze this catalog and produce the map of non-uniformity, which can then be compared to the given anisotropy function.

For example, let us set the parameters of anisotropy, or, more precisely, the parameters of the spatial distribution of axes of the radio sources (2) as follows: $\alpha_0 = 60°, \delta_0 = 45°, A = 3$. We distribute 10461 radio sources uniformly over the sky. The code generates a map of the distribution of simulated axes (Fig. 5) and a map of non-uniformity of histograms (Fig. 6a). As A > 0, the axis of anisotropy coincides with the domain of avoidance of the orientation of axes of the radio sources, implying that the negative extremum of the map (Fig. 6a) must be located near (α_0, δ_0). It is at this point that the map reaches its minimum (–161.8). In the plane perpendicular to the axis we see a dark contour corresponding to the domain of the preferred orientation, which also corresponds to the given anisotropy function. Such a clear pattern is not easy to discern in Fig. 5. The explanation is very simple: the search program is actually a strong filter suppressing low spatial frequencies, which is applied to the data used to build the map in Fig. 6a. An analysis of the noise of the simulated map for the isotropic case (A = 0) allowed us to coarsely estimate the aperture of this filter, which is about 90°. When applied to the map of the distribution of axes, such a filter yields a clear pattern (Fig. 6b), the structure of which reproduces the map in Fig. 6a. The filter improves the signal-to-noise ratio of the map, but at the same time, as it is evident from Fig. 3, it reduces the amplitude of anisotropy. Reversing the polarity of the anisotropy coefficient (A = −0.5), results, as it follows from formula (2), in a non-uniformity map with a positive extremum in the direction of the anisotropy axis (Fig. 6c). These numerical simulations lead us to a confident conclusion that the **anisoreal** code adequately describes the distribution of axes over the sky. We repeat our simulations with the same anisotropy parameters, but with the coordinates of real objects [9], the distribution of which reproduces the domain covered by the FIRST survey. As a result, we obtain the map of histogram non-uniformity (Fig. 6d), which differs from the map in Fig. 6a by a high non-uniformity in the domain of preferred orientation. The histogram of position angles counted with respect to the Celestial Pole also exhibits a strong non-uniformity and asymmetry. Repeated simulations for different samples of random numbers and anisotropy parameters showed that the nonuniform filling of the sky by radio sources leaves an indelible signature in the map of the histogram non-uniformity. The same effect explains the positive extremum in the experimental map in Fig. 1. A trivial conclusion follows: a program built to be used for estimating the anisotropy
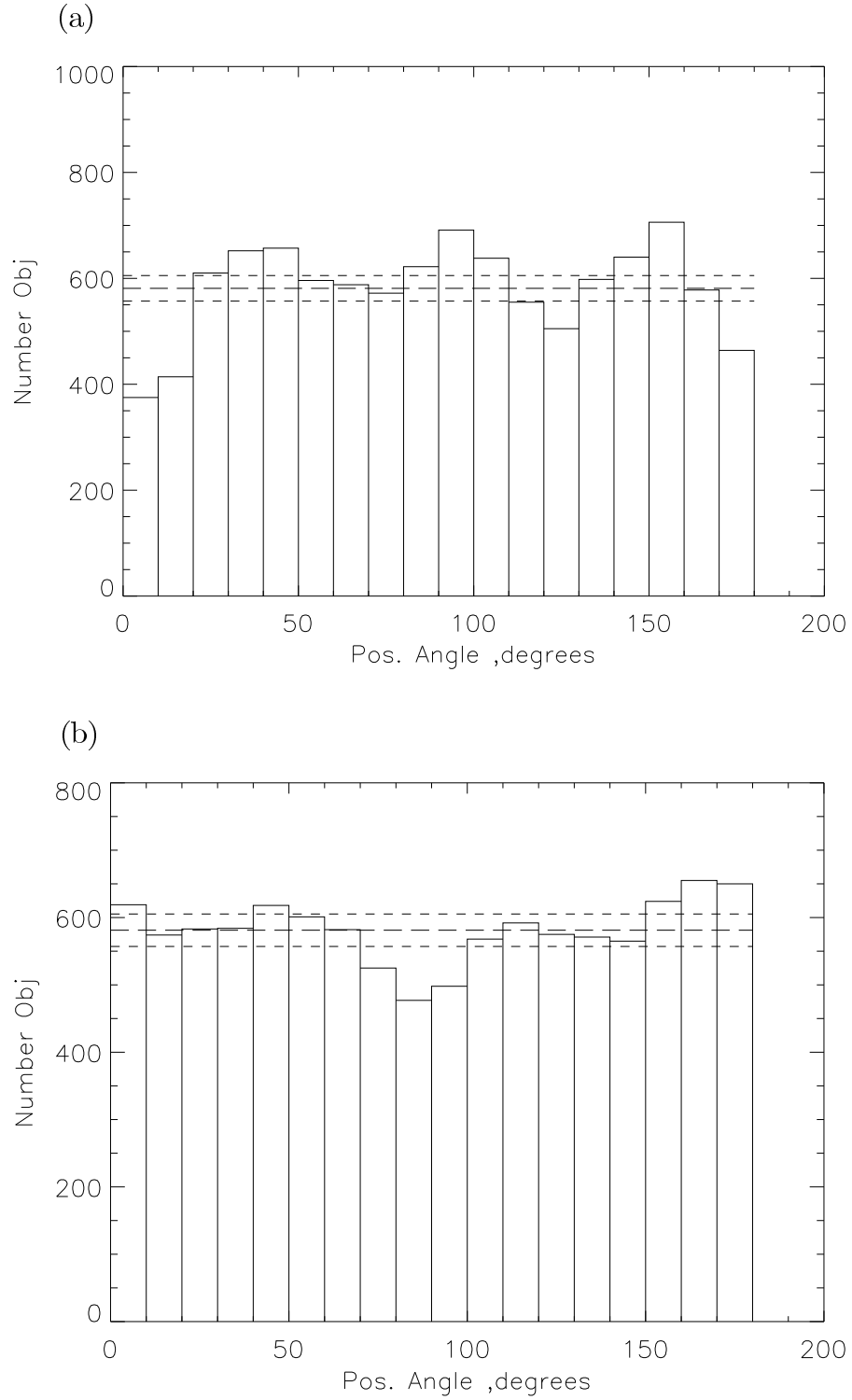
Figure 2. (a) The distribution of position angles with respect to the point of the negative extremum (120°, 80°); the non-uniformity of the histogram is 53.4. (b) The distribution of position angles with respect to the point of the positive extremum (140°, 0°); the non-uniformity of the histogram is 46.2.
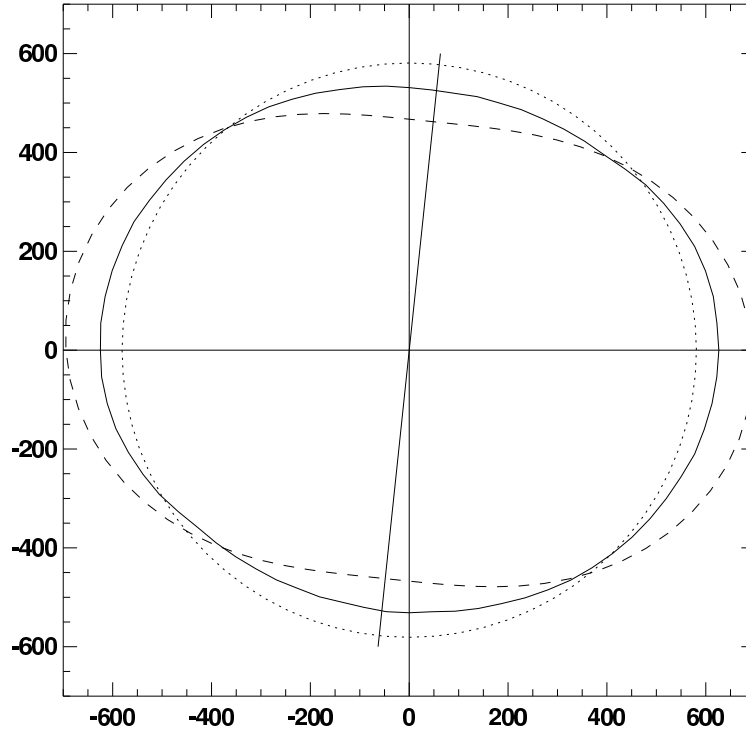
Figure 3. The cross section of the experimental map of non-uniformity (the solid line) and the distribution function of the radio sources' axes orientation. The dotted line corresponds to the isotropic distribution function for A = 0. The dashed line is the same function for A = 0.5. The angle between the anisotropy axis and the Y axis is equal to 6°.
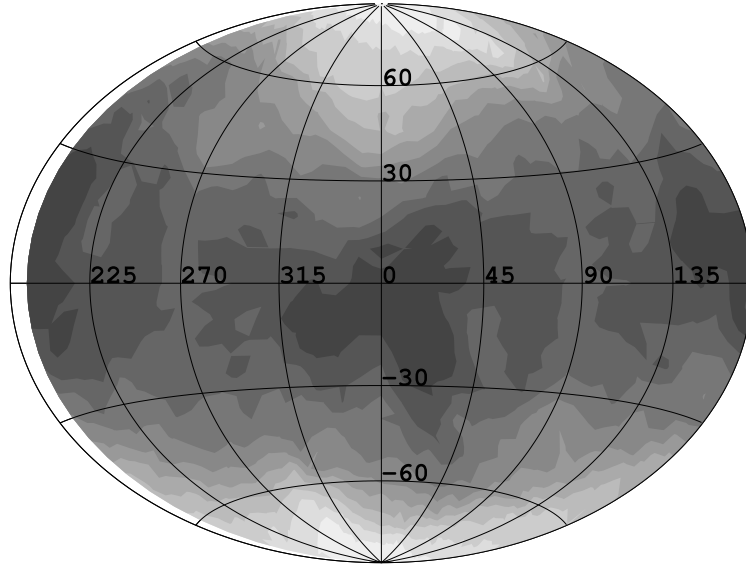
Figure 4. Experimental map of the non-uniformity of the FGC objects' normals' position angles distribution.

parameters must take into account the distribution of radio sources in the sky. Our attempt to construct an ideal analytical model yielded less reliable results.

4. PARAMETERS OF THE ANISOTROPY

To address our task, i.e., to try to find the parameters of anisotropy, using the most simple and natural method of manipulating the anisotropy parameters, α_0, δ_0, and A, and minimizing the residuals between
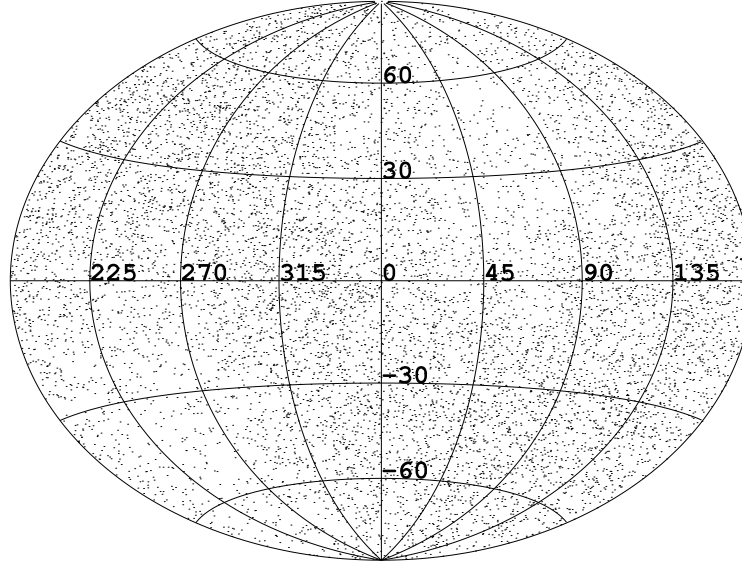
Figure 5. The map of the axes orientation of the radio sources from the simulated catalog. The axis of anisotropy points towards $\alpha_0 = 60°$, $\delta_0 = 45°$, A = 3. Radio sources are uniformly distributed over the sky.
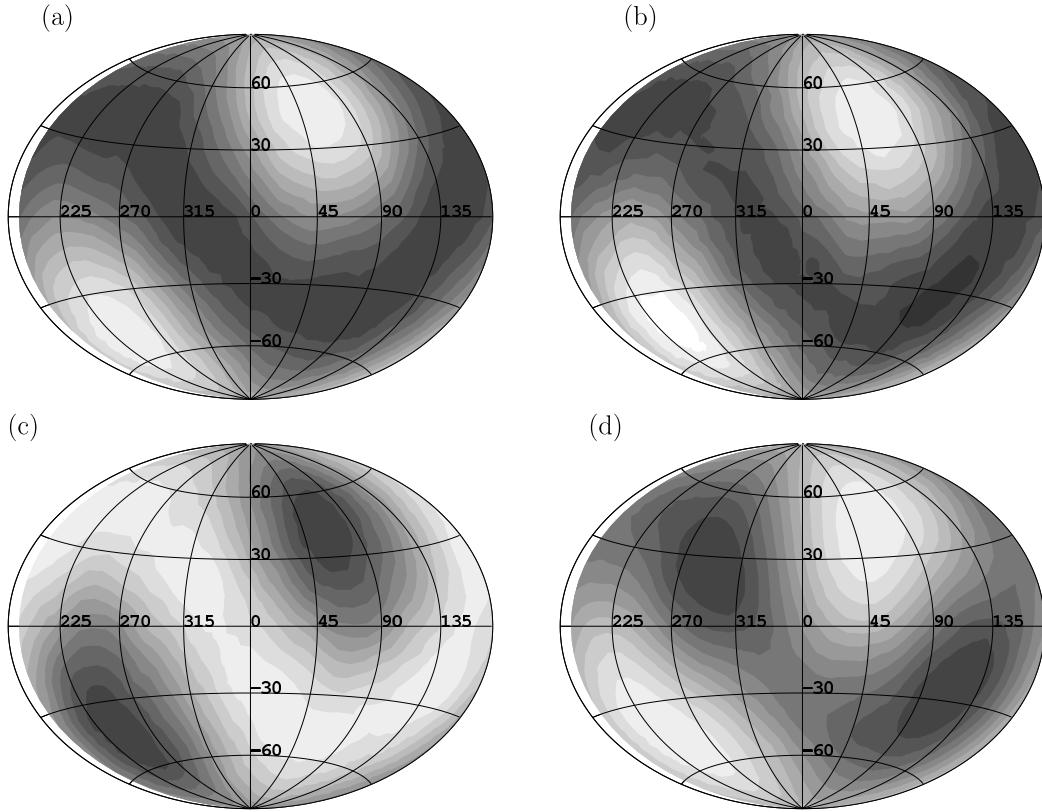

Figure 6. Maps of the non-uniformity of the position angles distribution of the radio sources from the simulated catalogs. (a) The axis of anisotropy points towards $\alpha_0 = 60°$, $\delta_0 = 45°$, A = 3. The radio sources are uniformly distributed in the sky. (b) The map of the radio sources axes orientation for the simulated catalog (Fig. 5) folded with a low-frequency spatial filter with an aperture of 90°. (c) The anisotropy axis points towards the point $\alpha_0 = 60°$, $\delta_0 = 45°$, A = −0.5. Radio sources are uniformly distributed over the sky. (d) The anisotropy axis points towards the direction $\alpha_0 = 60°$, $\delta_0 = 45°$, A = 3. Radio sources fill the domain of the FIRST survey—the coordinates of the radio sources are adopted from the catalog [9].

the simulated and experimental maps of histogram non-uniformity. We construct our model based on the actual distribution of radio sources over the sky. We perform this operation with several samples of random numbers in order to estimate not only the parameters, but also their errors. As a result, we infer the following anisotropy parameters:

$\alpha_0 = 180° \pm 92°$, $\delta_0 = 84° \pm 6°$, $A = 0.48 \pm 0.08$.

We use these very parameters in our cross section of the space distribution of angles in Fig. 3 (the dotted curve). The root-mean-square deviation between the isotropic distribution and the experimental map is equal to 29.3, and the root-mean-square deviation between the simulated and experimental maps is 6.9. The ratio of these standard deviations implies that the probability of the experimental distribution could be a randomly drawn sample of an isotropic distribution is $P < 0.00004$. We used the same programs to apply the above procedures to the catalog of edge-on galaxies [8] to obtain the following parameters of anisotropy:

$\delta_0 = 89°$, $A = 0.35$.

The right ascension (α_0) remains uncertain, since the point is close to the Celestial Pole.

The probability that the spatial distribution of the normals of galaxies is isotropic is less than 10^{-5}.

5. CONCLUSIONS

An analysis of extended radio sources position angles distribution showed that their axes are distributed anisotropically. The axes of radio sources avoid the direction towards the Celestial Pole and their preferred direction is towards the equator. The ratio of the probability densities of the orientation in these directions is close to 0.68. The same is true for the normals of the FGC catalog objects distribution, however, the corresponding ratio of probability densities is about 0.74. We cannot propose any mechanism that could result in such an alarming agreement of the directions of axes in both the optical and radio experiments. Numerical simulations show no software-related errors of such kind. The redshift distribution of 1801 radio sources of the catalog [9] leads us to cautiously conclude that the anisotropy extends out to $Z \sim 1$ or farther. The spatial distribution function must also undoubtedly have a finer structure in terms of locations and types of objects. To analyze this structure, more extensive catalogs and more sophisticated methods are required.

1. M. Reinhardt, Monthly Notices Roy. Astronom. Soc. **156**,151 (1972).
2. F. G. Brawn, Monthly Notices Roy. Astronom. Soc. **127**,517 (1963).
3. P. Nilson, Ann. Uppsala astron. Observ. **6**, 1 (1973).
4. P. Nilson, Rep. Uppsala astron. Observ. **3**, 1 (1974).
5. A. Lauberts, The ESO/Uppsala Survey of the ESO(B) Atlas (1982).
6. A. V. Mandzhos, A. Ya. Gregul', I. Yu. Izotova, and V. V. Tel'nyuk-Adamchuk, Astrofizika **26**, 321 (1987).
7. S. L. Parnovsky, I. D. Karachentsev, and V. E. Karachentseva, Monthly Notices Roy. Astronom. Soc. **268**, 665 (1994).
8. I. D. Karachentsev, V. E. Karachentseva, and S. L. Parnovsky, Astron. Nachr. **314**, 97 (1993).
9. V. R. Amirkhanyan, Astrophysical Bulletin **64**, 325 (2009).